Published in final edited form as:
Radiology. 1998 April ; 207(1): 91–102.

Alzheimer Disease: Quantitative H-1 MR Spectroscopic Imaging of Frontoparietal Brain[1]

Norbert Schuff, PhD, **Diane L. Amend, PhD**, **Dieter J. Meyerhoff, Dr rer nat**, **Jody L. Tanabe, MD**, **David Norman, MD**, **George Fein, PhD**, and **Michael W. Weiner, MD**
From the Magnetic Resonance Unit (N.S., D.L.A., D.J.M., J.L.T., M.W.W.) and the Department of Psychiatry Research (G.F.), Department of Veterans Affairs Medical Center; and the Departments of Radiology (N.S., D.J.M., J.LT., D.N., M.W.W.), Medicine (M.W.W.), Psychiatry (G.F., M.W.W.), and Neurology (M.W.W.), University of California at San Francisco, 4150 Clement St, 114M, San Francisco, CA 94121.

Abstract

PURPOSE—To replicate previous hydrogen-1 magnetic resonance (MR) spectroscopic imaging findings of metabolic abnormalities in patients with Alzheimer disease (AD), to verify that metabolic abnormalities are not an artifact of structural variations measured at MR imaging, to determine whether metabolic changes correlate with dementia severity, and to test whether MR imaging and MR spectroscopic imaging findings together improve ability to differentiate AD.

MATERIALS AND METHODS—MR spectroscopic imaging and MR imaging were performed in 28 patients with AD and 22 healthy elderly subjects. Spectroscopic imaging data were coregistered with MR imaging segmentation data to obtain volume-corrected metabolite concentrations.

RESULTS—Consistent with previous results, *N*-acetyl aspartate (NAA) levels were statistically significantly reduced in frontal and posterior mesial cortex of AD patients, presumably due to neuronal loss. NAA level reductions were independent of structural variations measured at MR imaging and, in parietal mesial cortex, were correlated mildly with dementia severity. Spectroscopic imaging findings of NAA level combined with MR imaging measures did not improve discrimination power for AD relative to that of MR imaging alone.

CONCLUSION—Reduced NAA levels in frontoparietal brain are of limited use for diagnosis of AD. However, they are not an artifact of structural variations and thus may provide useful information for the understanding of the pathologic processes underlying AD.

Index terms

Brain, diseases, 13.83; Brain, metabolism; Brain, MR, 13.121411, 13.12145, 13.12146; Dementia, 13.83; Magnetic resonance (MR), spectroscopy, 13.1215

[1]Supported by National Institutes of Health grant RO1 AG 10897. M.W.W. supported by the Department of Veterans Affairs Medical Research Service.

Address reprint requests to N.S.

Author contributions:
Guarantors of integrity of entire study, M.W.W., N.S.; study concepts and design, N.S., M.W.W.; definition of intellectual content, M.W.W.; literature research, N.S.; clinical studies, M.W.W., D.N., J.L.T.; experimental studies, N.S., D.J.M.; data acquisition, N.S., D.J.M., J.L.T.; data analysis, N.S., D.J.M.; statistical analysis, N.S., D.L.A., G.F.; manuscript preparation, N.S., M.W.W.; manuscript editing and review, N.S.

Neuroimaging is increasingly being used to aid in assessment of patients with dementia, including Alzheimer disease (AD). Magnetic resonance (MR) imaging of AD demonstrates accelerated total brain atrophy (primarily, loss of cortical gray matter; white matter volume remains largely unchanged) and greater enlargement of ventricular and sulcal cerebrospinal fluid (CSF) spaces, compared with signs of normal aging (1–3). Furthermore, MR imaging of the hippocampus in patients with AD has demonstrated marked volume loss (4). Positron emission tomography (PET) in patients with AD has demonstrated hypometabolism in the temporal and panietal association cortexes (5).

These anatomic and metabolic changes are of interest because they are presumably associated with the loss of neurons. However, neuronal loss in patients with AD is often accompanied by reactive gliosis (6) that attenuates tissue atrophy and affects cerebral metabolism to the degree that neurons are replaced by glia. Therefore, findings from MR imaging and PET may underestimate the extent of neuronal loss, which may account in part for the inability to diagnose AD reliably on the basis of MR imaging and PET results.

Hydrogen-1 MR spectroscopic imaging demonstrates the presence and concentration of the amino acid *N*-acetyl aspartate (NAA), which is specifically located in neurons but is absent in glia (7). In the presence of gliosis, NAA measured at H-1 MR spectroscopic imaging may be a more specific marker of neuronal loss than atrophy measured at MR imaging.

There have been numerous reports of reduced levels of NAA in various brain regions in patients with AD, which presumably reflects neuronal loss. In the first H-1 MR spectroscopic imaging study of AD at this laboratory (8), abnormalities were noted in metabolite ratios of NAA and choline- and creatine-containing compounds in white and gray matter of the centrum semiovale. In the white matter of patients with AD, the ratios of NAA to choline and NAA to creatine were reduced relative to those in control subjects in the absence of variations in the levels of choline or creatine; these results imply that decreased NAA was primarily responsible for these changes.

Decreased levels of NAA in white matter suggest diffuse axonal loss or damage. In the mesial gray matter of patients with AD, the NAA-to-choline ratio was lower, and the choline-to-creatine ratio was higher compared with those in control subjects, which implies that these changes could be due to decreased NAA and/or increased choline. Decreased NAA in gray matter suggests neuronal loss, whereas increased choline may be a result of membrane breakdown products.

In the second study at this laboratory (9), in which similar H-1 MR spectroscopic imaging methods were used, we extended the observation of metabolic abnormalities in the centrum semiovale to a larger population of patients with AD and control subjects; in addition, this second study included a group of patients with subcortical ischemic vascular dementia. Although the findings from the AD and control groups were similar to the findings from the first study, different metabolite changes were noted in patients with subcortical ischemic vascular dementia, which supported the possibility that H-1 MR spectroscopic imaging may provide information to help differentiate AD from subcortical ischemic vascular dementia.

Finally, in the third study at this laboratory (10), the extent to which these metabolic differences between patients and control subjects were independent of variations in the tissue composition of the MR spectroscopic imaging voxels (eg, enclosed amounts of gray matter, white matter, and high-signal-intensity white matter) was investigated. This analysis was made possible by using tissue segmentation information from MR imaging coregistered with the MR spectroscopic imaging data. Although the analysis revealed substantial variations in the tissue composition in the regions of interest, these changes did not contribute statistically significantly to the metabolite differences, which indicated that a reduced NAA-to-choline ratio and an

increased choline-to-creatine ratio in posterior mesial gray matter of patients with AD were not simply artifacts of these structural variations. Furthermore, MR spectroscopic imaging data combined with MR imaging segmentation data had a greater power to aid in correct classification of patients with AD and control subjects than either method had alone.

There were limitations to these studies, however, including relatively small numbers of subjects and an early MR imaging technology with which relatively (compared with today's standards) thick sections (5 mm) and intersection gaps (0.5 mm) were used, which compromised the accuracy of tissue segmentation. Furthermore, acquisition of the MR spectroscopic imaging data was performed at a relatively long echo time of 272 msec (because of technical imperfections of an MR imager equipped with unshielded gradient coils), which reduced sensitivity and increased signal dependence on T2 effects. Finally, in these previous MR spectroscopic imaging studies, we reported metabolite ratios, which are difficult to interpret, rather than concentrations.

Therefore, the present study had several goals. First, we aimed to replicate previous findings that suggested the presence of reduced NAA levels and increased choline levels by using improved H-1 MR spectroscopic imaging techniques in a new and larger population of patients with AD. In the present study, data were acquired with a shorter echo time (135 msec) to improve overall sensitivity and to reduce T2 dependency on the metabolite resonance intensities. In addition, the spectroscopic imaging data were expressed in terms of concentrations, to avoid use of metabolite ratios. Second, we sought to verify that these metabolic abnormalities are not simply artifacts of variations in the tissue composition of MR spectroscopic imaging voxels. This was accomplished by using MR imaging and semiautomated segmentation software to produce contiguous, 3-mm-thick sections across the entire brain. Third, we sought to determine if NAA level changes correlate with clinical measures of the severity of dementia in AD patients. Finally, we sought to test whether MR spectroscopic imaging variables together with MR imaging segmentation variables provide better discrimination between patients with AD and control subjects than MR imaging segmentation variables alone.

MATERIALS AND METHODS

Patients and Control Subjects

Twenty-eight patients (19 women and nine men [mean age ±1 standard deviation, 76.6 years ± 7.9; age range, 51–87 years]) with AD (24 probable, four possible) were included. In these patients, the diagnosis was established according to the criteria of the National Institute of Neurological and Communicative Disorders and the Alzheimer's Disease and Related Disorders Association (11). The patients had moderate to mild dementia, with a Folstein Mini-Mental State Examination (MMSE) (12) mean score (±1 standard deviation) of 19.1 ± 6.9 (range, 8–30). The diagnosis of possible AD in four patients was based on the observation that, at the time of evaluation, three had thyroid problems and the fourth had suspected complications with lifelong alcohol abuse.

The patient data were compared with results in 22 subjects with normal cognition; these subjects were on average 8.7 years younger (mean age, 67.9 years ± 7.3; age range, 52–85 years). For the purposes of analysis, the data from a subset of 17 AD patients and 17 control subjects of comparable age were first tested to determine the contribution of age to the MR spectroscopic imaging measures.

Initially, seven more patients and three more control subjects were enrolled in this study, but their data were not used for analysis because either the imaging acquisitions had to be

terminated prematurely because of the subject's request to be taken out of the magnet or data quality was severely degraded due to head movements during the acquisition.

All patients were recruited from the University of California at San Francisco Alzheimer Center; were examined by a neurologist; and underwent the standard battery of geriatric medical, neuropsychologic, psychiatric, and laboratory tests at the center. The 22 control subjects were recruited by posting flyers in community and retirement centers. They underwent an evaluation similar to that of the AD patients and were judged to have normal cognition. None of the patients or control subjects had evidence of stroke, cortical or subcortical infarctions, or other major abnormalities on MR images, which were read by a neuroradiologist (D.N.).

The study protocol was approved by the committee on human research at the University of California at San Francisco, and all subjects or their legal guardians gave written informed consent before participation in the study.

MR Imaging and MR Spectroscopic Imaging

All studies were performed with a 1.5-T system (Magnetom Vision; Siemens Medical Systems, Iselin, NJ) equipped with a standard quadrature head coil. The combined MR imaging and MR spectroscopic imaging examination lasted approximately 45 minutes and was completed by all patients and control subjects included in this study. To minimize motion of the participant's head, a vacuum-molded head holder (Vac-Pac; Olympic Medical, Seattle, Wash) was used to restrict head movements. Sagittal T1-weighted localizer MR images (repetition time msec/echo time msec, 240/6) and oblique axial double spin-echo MR images (3,000/20, 80; 1.0 × 1.4-mm resolution) angulated along the plenum sphenoidale (as seen on the localizer image) were acquired. To cover the entire brain from the inferior cerebellum to the vertex, 48–52 contiguous 3-mm-thick sections were acquired.

H-1 MR spectroscopic imaging data sets were acquired by using a spin-echo two-dimensional MR spectroscopic imaging sequence (1,800/135) with preselection of a region of interest (point-resolved spectroscopic volume), which necessitated a total acquisition time of approximately 13 minutes. The point-resolved spectroscopic volume was angulated parallel to the double spin-echo imaging plane and was positioned immediately superior to the lateral ventricles as seen on the localizes image. Because of the different shape of the lateral ventricles in the participants, the point-resolved spectroscopic volume included a small fraction of the ventricles, in some cases. The anteroposterior (length) and right-left (width) dimensions of the point-resolved spectroscopic volume (mean length, 105.3 mm; mean width, 71.1 mm) were adjusted on axial MR images in every participant, according to the brain size. Section thickness was constant at 15 mm. Typical angulation and position of a point-resolved spectroscopic volume are depicted in Figure 1. The MR spectroscopic imaging field of view was 210 × 210 mm and was sampled by using a reduced k-space sampling scheme over a circularly restricted region equivalent to a maximum of 24 × 24 phase-encoding steps (13), which resulted in a nominal MR spectroscopic imaging spatial resolution of 0.8 × 0.8 mm. The spectral sweep width was 1,000 Hz.

MR Image Segmentation

Semiautomated, interactive computer segmentation of the MR images into specific tissue and anatomic compartments was performed by using software developed at our institution by one of the authors (G.F.). All brains were segmented on images into areas of ventricular CSF, sulcal CSF, cortical and subcortical gray matter, white matter, and hyperintense white matter.

Two trained operators (D.L.A., J.L.T.), both blinded to the participants' identity, processed the MR images. Editing of sub-cortical gray matter and hyperintense white matter regions was performed by one operator (J.L.T.). All values were normalized to the total number of pixels, expressed as a percentage of the intracranial volume. Reliability of image segmentation was evaluated by one of the authors (G.F.), who used a total of 20 segmentation images in 10 control subjects. The control subjects underwent imaging twice, and images 1 and 2 in each subject were segmented by a different operator. The coefficient of variation was 1.9% of the mean value for gray matter and 2.3% of that for white matter, which indicated that the accuracy of the segmentation measurement was far better than the intersubject variance, which typically was approximately 11% for gray matter and 8% for white matter. The interclass correlation coefficient was .961 for gray matter and .937 for white matter, which demonstrated that gray and white matter segmentation is practically independent of interoperator variations. Additional details about the segmentation procedure are available in reference 3.

MR Spectroscopic Image Analysis

After acquisition, the MR spectroscopic imaging data were zero filled to a rectangular matrix of 32 × 32 × 1,024 points, were Fourier transformed, and were phase- and baseline-corrected by using software developed at our institution (14). Four-hertz Gaussian line broadening was used in the spectral direction, and mild Gaussian filtering was applied along the spatial directions to reduce Gibbs ringing effects, which resulted in an effective MR spectroscopic image resolution of approximately 1.1 × 1.1 mm. Spectra were extracted from nine regions of interest (voxels) within the point-resolved spectroscopic region by following guidelines described in detail by Meyerhoff et al (8).

The size and typical location of the selected voxels are shown in Figure lb. Six lateral voxels were selected: two each in the frontal, middle, and posterior regions of the centrum semiovale (predominantly white matter). The remaining three voxels were selected from the midline of the brain: one each from a region of frontal, middle, and posterior mesial cortex (predominantly gray matter).

The MR resonances from NAA, creatine, and choline were curve fitted by using NMR1 software (New Research Methods, Syracuse, NY). Voxel selection and spectral fitting were performed by one trained operator (DJ.M.), who was blinded to the diagnosis in the participants. To estimate concentrations in milligrams per liter, the integral values of the metabolite resonances were referenced to values obtained from a head-sized phantom and included corrections for coil loading, receiver gain, and metabolite T1 and T2 by using previously reported (15) MR spectroscopic T1 and T2 values in healthy elderly subjects. It was assumed that the metabolite relaxation rates were the same for AD patients and control subjects and for gray and white matter.

To verify that metabolic changes were not an artifact of variations in the tissue composition of MR spectroscopic imaging voxels, tissue enclosed in each voxel was analyzed for amounts of gray matter, white matter, hyperintense white matter, and CSF by using software developed at our institution. This computation used the tissue-segmented MR images coregistered with MR spectroscopic imaging data and was performed with consideration of the MR spectroscopic imaging point-spread function, chemical shift displacements, and the signal sensitivity profile of the point-resolved spectroscopic volume, which was determined experimentally by using a head-sized phantom. The tissue content ρ in each voxel was estimated with the following equation: $\rho = gm + wm + wmsh$, where gm, wm, and wmsh represent the enclosed amounts (ie, the number of pixels from the segmented MR images) of gray matter, white matter, and hyperintense white matter, respectively.

With the assumption that metabolite resonances are not detected in CSF, volume-corrected metabolite integrals were then computed by using metab = $metab_u/\rho$, where metab and $metab_u$ are the corrected amount and uncorrected amount, respectively, of the metabolite. All MR spectroscopic metabolite values presented in this study are volume-corrected. Furthermore, the tissue composition in each voxel was characterized by computing tissue fraction factors for gray matter (X_{GM} = gm/ρ), white matter (X_{WM} = wm/ρ), and hyperintense white matter (X_{WMSH} = wmsh/ρ). For example, X_{GM} is 1.0 for a voxel with pure gray matter and 0.0 for a voxel with white matter and hyperintense white matter but without gray matter. These factors were used as covariates for the statistical analysis to determine the extent to which the tissue composition contributed to metabolic differences.

Statistical Analysis

Because the AD patients in this study were on average statistically significantly older than the control subjects, metabolite differences between the groups were first tested in a subset of patients and subjects of comparable age to minimize age effects. The Student *t* test was used to test for differences in the age distribution between groups.

Tests of metabolite differences between patients and control subjects were performed separately for the voxels from the mesial cortex and lateral centrum semiovale in frontal, middle, and posterior brain, which resulted in a total of six comparisons. Metabolite differences between groups by tissue and region were tested with repeated-measures analysis of variance with the Bonferroni correction for multiple comparisons. Analysis of variance was used to test whether metabolite changes were statistically significantly different between male and female participants within each group. Finally, analysis of covariance was used to test whether the metabolite differences would remain statistically significant after adjustment for differences in the tissue composition of the MR spectroscopic imaging voxels.

Once the statistically significant metabolite differences between patients and control subjects were identified in the subset, the analysis was extended to include data from the rest of the study population, and between-group differences were tested in a post-hoc manner. Initially, the relationship between metabolite changes and age was determined separately for patients and control subjects by using an analysis of covariance. If age did not contribute significantly to metabolite changes, we continued the analysis of covariance to test whether metabolite differences between groups would remain significant after adjustment for variations in the tissue composition of the voxels. If age contributed significantly to the metabolite differences, the data were not further considered for analysis because it would not have been possible to distinguish changes related to AD from those associated with age.

Linear relationships between MR spectroscopic imaging or MR imaging segmentation variables and MMSE scores in AD were tested with the Pearson product-moment correlation. Linear discriminant-function analysis was used to determine which MR imaging and MR spectroscopic imaging variables or combination of variables discriminated best between AD patients and control subjects. Results are expressed as means ± the standard error of the mean, unless otherwise indicated.

RESULTS

Demographic Data

Table 1 lists the demographic data of the study population, together with the data of the selected subset of 17 AD patients and control subjects of comparable age. In the total study population, the mean age (±1 standard deviation) of the AD patients was 76.6 years ± 7.9, and that of the control subjects was 67.9 years ± 7.3; this age difference was statistically significant (*P* = .

002). In the subset, the mean age of the AD patients was 73.0 years ± 8.0, and that of the control subjects was 69.5 years ± 7.6; this difference was not significantly different ($P = .2$). In the total study population, the AD patients and control subjects were 51–87 years of age and had a similar number of years of education. Nineteen (68%) of the 28 AD patients and 10 (45%) of the 22 control subjects were women. The patients reported an average duration (±1 standard deviation) of their symptoms related to AD of 4.3 years ± 2.3. The mean MMSE score (±1 standard deviation) in AD patients was 19.1 ± 6.9 (score range, 8–30), which was significantly lower ($P < .001$) than that in the control subjects (mean, 29.5 ± 0.9).

In comparison with the total group of AD patients in this study, the 17 AD patients in the subset were an average 3.6 years younger. The percentage of women in the AD subgroup further increased from 68% to 76% (13 of 17), while other demographic data did not change substantially. In comparison with the entire control group, the 17 control subjects in the subset were on average 1.6 years older and included a larger percentage of women (59% [10 of 17]), while other demographic data were virtually unchanged.

MR Spectroscopic Imaging Results

Table 2 lists the mean concentrations of volume-corrected NAA, creatine, and choline from the mesial cortex and the centrum semiovale in frontal, middle, and posterior brain of the subset of AD patients and control subjects. The most prominent differences between AD patients and control subjects were lower levels in AD patients of NAA in the frontal mesial cortex and centrum semiovale and in the posterior mesial cortex. In the frontal brain in AD patients, NAA was reduced (relative to that in control subjects) by 14.0% in the mesial cortex ($P < .03$) and by 9.8% in the centrum semiovale ($P < .003$). In the posterior brain in AD patients, NAA was reduced (relative to that in control subjects) by 10.4% in the mesial cortex ($P < .03$), whereas in the centrum semiovale the difference was not statistically significant. In the middle brain of AD patients, NAA levels in both the cortex and the centrum semiovale were similar to those in control subjects.

The NAA levels were not significantly different between women and men in either the patient group or the control group. In contrast to the changes in NAA level, neither choline nor creatine levels were significantly different in any brain region in AD patients compared with the levels in control subjects.

MR imaging segmentation results from the age-matched cohort have been reported elsewhere (3). In that previous study, AD patients had a 10% decrease in cortical gray matter volume relative to the volume in control subjects ($P < .0001$) and an 88% increase in hyperintense white matter volume ($P < .005$); white matter volume did not change significantly.

One would expect that these structural changes are also reflected in the tissue composition of the selected MR spectroscopic imaging voxels, which could mimic metabolic differences if no adjustments are made. Table 3 lists the tissue composition of the MR spectroscopic imaging voxels corresponding to the regions listed in Table 2. Overall, voxels in the frontal and posterior mesial cortex in AD patients enclosed significantly ($P < .005$) less gray matter (up to 13%) and, consequently, more white matter than voxels from the corresponding region in control subjects, presumably because of larger gray matter loss in patients with AD. Furthermore, voxels from centrum semiovale white matter in AD patients contained more hyperintense white matter than those in controls, especially in frontal white matter, where the difference between the groups reached 120% ($P < .0001$).

To test whether the NAA differences were independent of differences in voxel tissue composition, analysis of covariance was performed by using the tissue fraction factors for gray matter (X_{GM}) and hyperintense white matter (X_{WMSH}) of each voxel as covariates. In the frontal

and posterior mesial cortex, NAA differences between the groups remained significant ($P < .03$) and variations of the tissue fraction factor for gray matter did not contribute significantly ($P < .2$) to the difference, which suggests that NAA reductions in these regions in AD patients are not simply an artifact of variations in the tissue composition of the voxels. Similarly, NAA differences between AD patients and control subjects in anterior centrum semiovale white matter remained significant ($P < .003$), and contributions from the tissue fraction factor for hyperintense white matter differences were not significant ($P > .09$), which suggests that increased hyperintense white matter in AD patients was not primarily responsible for the NAA difference.

Next, we extended the analysis of MR spectroscopic imaging data to the remaining 11 AD patients and five control subjects (but now restricted to the regions of frontal and posterior mesial cortical gray matter and frontal centrum semiovale white matter).

Because the AD patients were statistically significantly older than the control subjects, we first tested whether NAA changes in these regions were correlated with age. Over the age range studied, the NAA changes in AD patients were not statistically significantly ($P > .1$) related to age ($r = -.17$ for the frontal mesial cortex; $r = -.11$ for the posterior mesial cortex; $r = -.09$ for the frontal centrum semiovale). Similar non-statistically significant ($P > .1$) results were obtained in control subjects ($r = .15$ for the frontal mesial cortex; $r = -.10$ for the posterior mesial cortex; $r = -.13$ for the frontal centrum semiovale). Furthermore, analysis of covariance results showed that age did not contribute significantly to NAA level differences between the groups at the different brain regions ($P > .3$ for all regions), which indicates that NAA level variations cannot simply be explained in terms of age effects.

Table 4 lists the mean NAA concentrations in frontal, middle, and posterior brain regions from the entire study population of AD patients and control subjects. Table 5 lists the tissue compositions of the voxels corresponding to the brain regions listed in Table 4. NAA level in the mesial cortex remained reduced in AD patients compared with that in control subjects; this reduction was 11.1% ($P < .02$) for the frontal region and 9.8% ($P < .02$) for the posterior region. Furthermore, these NAA level differences between the groups remained significant after adjustment for variations in the tissue fraction factor for gray matter in these regions.

In contrast to mesial cortex, NAA differences in the frontal centrum semiovale between AD patients and control subjects were not independent of differences in the hyperintense white matter composition of the MR spectroscopic imaging voxels. In this case, between-group differences in hyperintense white matter amounts enclosed in the MR spectroscopic imaging voxels contributed significantly ($P < .01$) to the NAA level differences, which suggests that reduced NAA level in frontal centrum semiovale white matter of AD patients is primarily an artifact of increased hyperintense white matter.

This finding led us to investigate further the relationship between metabolite variations and tissue types. Figure 2a, 2b, and 2c display the variations of NAA, creatine, and choline levels, respectively, in AD patients and control subjects as a function of the amount of gray matter enclosed in the selected voxels.

In control subjects, NAA levels increased modestly but significantly with increased amount of gray matter ($r = .35$; $P < .02$), which indicates the presence of higher concentrations of NAA in gray matter than in white matter. In contrast to the findings in control subjects, NAA levels in AD patients were not significantly correlated with the amount of gray matter ($r = .17$; $P > .1$), which suggests that there are similar levels of NAA in white and gray matter, presumably because NAA reductions in cases of AD occur primarily in gray matter and less so in white matter.

Changes in creatine levels were positively correlated with the amount of gray matter in both AD patients ($r = .59$; $P < .01$) and control subjects ($r = .63$; $P < .01$), which indicates that there are higher levels of creatine in gray matter than in white matter. No significant correlation was found between choline and the amount of gray matter, which suggests that there are similar levels of choline in gray and white matter.

Finally, Figure 2d depicts the relationship of NAA level changes in AD patients and control subjects with the amount of hyperintense white matter enclosed in the MR spectroscopic imaging voxels. In AD patients, NAA levels decreased significantly with increases in the amount of hyperintense white matter ($r = .49$; $P < .01$), which indicates that NAA level is reduced in hyperintense white matter compared with the level in normal white matter. This correlation seemed to be less prominent in control subjects; however, only a few voxels with large amounts of hyperintense white matter were available in the control subjects, and the determination of the correlation was therefore less accurate.

Neither creatine nor choline level showed a significant correlation with the amount of hyperintense white matter. Overall, these results demonstrate the importance of accounting for variations in voxel tissue composition when one is analyzing H-1 MR spectroscopic imaging data.

We further tested whether reductions in NAA level in frontal or posterior mesial cortex of AD patients were related to the severity of dementia. Figure 3 depicts the changes in NAA level in the frontal and posterior mesial cortex of 26 AD patients as a function of dementia severity (MMSE score). (Two AD patients did not undergo the MMSE because they were not English speakers.) A weak but significant correlation was found between changes in NAA level in the posterior mesial cortex and severity of dementia ($r = .42$; $P = .03$), which suggests that the NAA level in this region may reflect some forms of cognitive impairment. No significant correlation between NAA level and dementia severity was found for the frontal mesial cortex ($r = .19$,$P > .3$).

We also tested whether MR imaging segmentation variables were correlated with dementia severity. The percentage of sulcal CSF correlated significantly with severity of dementia in the AD group ($r = -.46$; $P < .03$), but correlation between other segmentation variables and dementia severity were not significant (percentage cortical gray matter, $r = .38$, $P > .1$; percentage of ventricular CSF, $r = -.18$, $P > .1$).

Finally, we tested the discrimination power of variables from MR imaging segmentation, from MR spectroscopic imaging, and from the combination of both to correctly classify AD patients and control subjects by using linear discriminant-function analysis. The percentage of cortical gray matter was chosen as the MR imaging variable for the discrimination model because our previous MR imaging results (3) showed that total cortical gray matter loss provided the best performance in aid of the diagnosis of AD in comparison with other measures of morphologic changes (eg, ventricular and sulcal CSF enlargement). Mean NAA level in frontal and parietal gray matter was chosen as the MR spectroscopic imaging variable because NAA levels in these regions were significantly reduced in AD patients. The analysis was performed with results in 26 AD patients and 17 control subjects in whom complete sets of MR spectroscopic imaging and MR imaging data were acquired.

Figure 4 depicts the distributions of the percentage of gray matter (Fig 4a), NAA concentration (Fig 4b), and the product of both variables (Fig 4c) in AD patients and control subjects. The 95% confidence intervals for each of the variables in the control group demonstrate that neither variable alone nor their combination is sufficient to help completely distinguish AD patients from control subjects. The percentage of cortical gray matter and NAA level can also be graphically compared in Figure 2a, which indicates a substantial overlap between both groups.

Linear discriminant-function analysis revealed that the percentage of cortical gray matter enabled correct classification of 20 (77%) of the 26 AD patients and 15 (88%) of the 17 control subjects, for a combined correct classification percentage of 81% (35 of 43 participants). NAA level in the mesial cortex enabled correct classification of 21 (81%) AD patients but of only 11 (65%) control subjects, for a combined correct classification percentage of 74% (32 participants). When the product of percentage cortical GM and NAA level was used, correct classification was achieved for 21 (81%) AD patients and 13 (76%) control subjects, for a combined correct classification percentage of 79% (34 participants), which was similar to the classification percentage achieved with MR imaging variables alone.

DISCUSSION

There were five major findings in this study. First, NAA levels were decreased in frontal and posterior mesial cortex and in frontal centrum semiovale in AD patients compared with NAA levels in control subjects, but the levels of choline- and creatine-containing metabolites were not statistically significantly different. Second, reductions in NAA levels in AD patients cannot be explained in terms of structural variations as measured at MR imaging, because NAA measures were volume corrected, and variations of the voxel tissue composition did not statistically significantly contribute to changes in NAA levels. Third, NAA levels in control subjects increased with increases in amount of gray matter enclosed in the MR spectroscopic imaging voxels, which suggests the presence of higher NAA levels in gray matter than in white matter. This correlation was not observed in AD patients, presumably because reductions in NAA levels in AD patients occurred predominantly in gray matter and less so in white matter. Furthermore, NAA level was inversely correlated with the amount of hyperintense white matter, which suggests the presence of decreased NAA levels in white matter lesions. Fourth, NAA level in the parietal mesial cortex of AD patients was correlated with dementia severity (MMSE score). Fifth, NAA level measured with MR spectroscopic imaging did not result in improved classification power compared with percentage of cortical gray matter loss measured with MR imaging.

Our first major finding of reduced NAA levels in frontal and parietal gray and white matter confirms results of several previous studies from this (8–10) and other laboratories (15,16). Contrary to results from most previous studies, in which metabolite ratios were used, our results demonstrate that NAA concentrations are reduced, which is in agreement with the quantitative results from a single-voxel H-1 MR spectroscopy study of Moats et al (15). If it is assumed that NAA is present only in neuronal bodies and axons (17), reduction of NAA concentration strongly suggests reduction of the volume ratio of neuronal to nonneuronal cells. Because neuronal loss (necrosis) or volume reduction (eg, loss of dendritic connections) in AD is often accompanied by reactive gliosis (6), this is the likely explanation for decreased NAA levels in AD patients.

It has been previously shown (18) that acute insults such as ischemia or inflammation can lead to reversible decreases in NAA levels, which appear to be due to transient neuronal metabolic disturbances. It is possible, therefore, that reductions in NAA levels in AD patients do not necessarily indicate neuronal loss but reflect potentially reversible metabolic abnormalities. AD is, however, a slowly progressive degenerative disease, and it is not characterized by acute inflammation or ischemia. Hence, this possible explanation for NAA level reductions in AD appears to be less likely.

Finally, it is possible that T1 or T2 changes were responsible for NAA signal intensity decreases. However, Christiansen et al (16) reported increased T2 values for NAA in the frontal lobe of AD patients. Increased T2 would tend to increase signal intensity, especially at relatively long echo times. This raises the possibility that increased T2 may have offset the

NAA signal intensity decreases, and the extent of neuronal loss may therefore be underestimated by changes in NAA level. Because of the considerable amount of additional time needed for the subjects to remain in the magnet, it was not possible to perform relaxation time measurements in the current study.

The current results showed no statistically significant changes in levels of choline- or creatine-containing metabolites. The absence of changes in choline measurements in AD patients differs from findings suggestive of increased choline levels in AD patients in our previous studies (8,9), in which metabolite ratios were used, and in others' studies (19). Similar to us, however, authors of other quantitative studies (15,20) found no evidence of increased choline levels in AD patients.

There are several possible explanations for these contradictory results, including differences in relaxation times, regional variations, and heterogeneity of the patient population. A first possibility is that changes in choline levels in AD patients are due primarily to variations in T1 and T2. MR spectroscopic imaging in this study was performed at a shorter echo time (135 msec) than that used (272 msec) in our earlier studies (8,9). If the choline level increase observed previously in AD patients was due to a T2 prolongation of the choline resonance, then it is possible that this increase would remain undetected at examination with the shorter echo time used in this study. However, Huang et al (21) reported increased choline level in AD patients examined with an echo time as short as 30 msec. Furthermore, preliminary measurements of T1 and T2 revealed similar values in T2 for choline in AD patients and elderly individuals with normal cognition (15). Therefore, relaxation time differences do not appear to account totally for the discrepant findings of choline level changes in AD patients.

A second possibility is that regional variations in choline concentrations may account for the discrepancy. For example, Huang et al (21) found increased levels of choline only in the primary visual cortex of AD patients but not in the left and right parietal cortexes.

Finally, heterogeneity of the patient population is another possibility that may account for the discrepancy. People with AD have different genotypes for apolipoprotein E, which pose different degrees of risk for development of AD. In addition, some isoform-specific interactions between apolipoprotein E and pathologic lesions have been demonstrated in patients with AD (22). This raises the possibility that, in cases of AD, differences in apolipoprotein E may account for differences in the metabolism of membrane phospholipids (23) that regulate the structure and stability of membranes. Such differences might thus be reflected as differences in concentrations of choline-containing membrane molecules, which are detected as an increase in choline level at H-1 MR spectroscopic imaging. Apolipoprotein E data were not available in the patients included in this study; therefore, such a subtype analysis could not be performed.

Our second major finding was that NAA reductions in frontal and posterior gray matter of AD patients cannot be explained in terms of structural variations measured at MR imaging. This analysis was made possible by using information from coregistered MR imaging segmentation data, which were reported earlier by Tanabe et al (3). Our analysis also replicated previous MR spectroscopic imaging results from this laboratory by MacKay et al (10). However, the accuracy of image segmentation data was compromised in the study by MacKay et al, because MR images were not obtained from contiguous sections and did not cover the entire brain.

This result is important because it documents that changes in NAA levels in AD patients are not simply a reflection of differences in the tissue composition of MR spectroscopic imaging voxels. This result also suggests that changes in NAA levels provide information in addition to that acquired at MR imaging, which may be used to improve diagnostic classification. Furthermore, these results emphasize the value of MR imaging segmentation data for analysis and interpretation of H-1 MR spectroscopic imaging data, and we suggest that this approach

may be used to improve analysis of data from other MR spectroscopic studies. For example, our analysis revealed that reductions in NAA levels in frontal white matter of AD patients were simply an artifact of increased hyperintense white matter in this region, which provided no information in addition to that already available from MR imaging.

The third finding was that changes in NAA levels in control subjects correlated with the amount of gray matter enclosed in the MR spectroscopic imaging voxels, which suggested the presence of higher NAA levels in gray matter than in white matter. This result is consistent with those of previous studies by Hetherington et al (24) in nonelderly control subjects and by Lim et al (25) of normal aging, both of whom used regression analysis to predict NAA concentrations in pure gray and pure white matter, with higher levels seen in gray matter than in white matter. Unlike in the control subjects in our study, we found no correlation between NAA levels and the amount of gray matter in AD patients, which indicated the presence of similar NAA levels in both gray and white matter, presumably because of reduced NAA levels in the gray matter of AD patients.

It is possible that the prominent reductions of NAA levels in AD patients' gray matter but not in white matter reflect the fact that cortical neurons are directly involved in the pathologic process of AD. The correlation of NAA level changes with voxel tissue composition also showed that NAA levels are decreased in regions with hyperintense white matter, which is consistent with previous reports (26) from this laboratory. As completely automated spectral fitting programs become more widely available, it will be possible to correlate the metabolite concentration with the measured tissue composition for each voxel on images of the brain. This approach would be expected to provide additional information and possibly to increase discriminative power for differentiation of various diseases.

The fourth major finding was that NAA levels in parietal mesial cortex in AD patients showed a weak but statistically significant correlation with MMSE score. No correlation was found between MMSE score and NAA levels in frontal gray matter. This result is consistent with the concept that neuronal loss in the parietal lobe is chiefly responsible for the impairment of some cognitive functions in patients with AD. Others (20,21) have also reported a correlation of NAA levels with dementia severity. This result is encouraging because it supports the suggestion that NAA level reductions are associated with diminished brain function, presumably precipitated by means of neuronal loss or volume reduction (eg, loss of dendritic connections). In addition, this result emphasizes the possibility that sequential measurements of NAA levels may be a useful and objective means to document the progression of AD and the results of treatment.

Of the image segmentation variables, only the percentage of sulcal CSF showed a weak but statistically significant correlation with severity of dementia. Perhaps both NAA level and percentage of sulcal CSF, more than the other measures, closely reflect neuronal loss resulting in cognitive impairment.

The fifth finding was that changes in NAA levels in mesial cortex did not improve the classification power relative to percentage of cortical gray matter loss. This finding does not support the results from our previous study (10) of the frontoparietal brain, which suggested that combinations of MR imaging and H-1 MR spectroscopic imaging findings improve classification power relative to the use of either measure alone. That previous study was limited because of a small sample size (six AD patients, 11 control subjects), use of a relatively long echo time (272 msec) at spectroscopic imaging, and acquisition of MR images with an intersection gap that thereby excluded up to 30% of the brain. In the present study, we included 4.3 times more patients and 1.5 times more control subjects, acquired spectroscopic imaging data with a much shorter echo time (135 msec), and obtained MR images contiguously across

the entire brain. These differences—especially the larger sample size, which increased the possibility of greater phenotypic heterogeneity of AD—may explain the discrepancy between findings from this study and those from the earlier one.

There are several limitations to the present study. A first limitation is that H-1 MR spectroscopic imaging was performed in a frontopanietal region of the brain, which is not necessarily the region known to be most affected by AD. The greatest changes in AD are expected in the hippocampus and temporal lobe, as well as in regions of the surface cortex of the frontal and parietal lobes. These brain regions were not accessible with MR spectroscopic imaging at the time this study began. Subsequently, techniques have been developed to perform H-1 MR spectroscopic imaging of the hippocampus and mesial temporal lobe regions, in which striking NAA level reductions have been found in the hippocampal region of patients with epilepsy (27). Other results (28) from this laboratory have shown reduced NAA levels in the hippocampal region of AD patients. In addition, we documented that these NAA level reductions were to a large extent independent of hippocampal volume loss measured at MR imaging and contributed substantially to the discrimination of AD patients from control subjects, in contrast to the finding in the present study.

Furthermore, we (29) and others (30) have developed new multisection H-1 MR spectroscopic imaging techniques that facilitate study of metabolic changes in large sections of the brain, including surface cortex. These techniques make use of outer-volume suppression pulses (30), lipid nulling (31), or data processing techniques (29) to reduce interference of the cortical metabolite signals with strong resonances from subcutaneous lipids. Recently, Tedeschi et al (32) performed multisection H-1 MR spectroscopic imaging in patients with AD and found marked changes in NAA metabolite ratios in the associative cortexes, similar to the pattern of metabolic decrements reported in a number of PET studies (5).

A second limitation of this study was that the echo time we used was still too long for the measurement of *myo*-inositol, which has been shown to be elevated in cases of AD (33) and other conditions, including Creutzfeldt-Jakob disease (34) and frontotemporal dementia (20). Shonk et al (35) have further reported that the ratio of *myo*-inositol to NAA can be used to clearly discriminate patients with AD from healthy elderly individuals. Furthermore, Ernst et al (20) examined patients with AD and those with frontotemporal dementia and found elevated *myo*-inositol levels in the temporopanietal cortex of AD patients, whereas these levels were elevated in the frontal cortex in patients with frontotemporal dementia; this result suggested the possibility that findings of *myo*-inositol level may be useful for differentiation of these two conditions.

Multisection H-1 MR spectroscopic imaging with an echo time of 20–30 msec, with which detection of regional changes of *myo*-inositol levels is possible, has been performed (36), but at the expense of greater lipid contamination of the metabolite resonances. In the future, techniques should be developed that use multisection or three-dimensional acquisition to depict regional changes in levels of NAA and other metabolites (including *myo*-inositol) in multiple brain regions. It is expected that the ability to sample many areas of the brain and observe a number of different metabolites, which change in dementia, will lead to improved discriminative power to identify AD.

Recently, other groups (25,31) have developed automated spectral analysis software to evaluate MR spectra from a large number of voxels, which eliminates the highly subjective approach of voxel selection from discrete regions. Although an automated spectral analysis program is under development at this laboratory, it was not available at the time of this study.

A potential source of bias in this study could be the difference in the distribution of sex and age between the groups. Despite an imbalance in the number of women and men in the groups,

analysis of covariance demonstrated no group effect attributable to sex. The effect of sex on changes in NAA levels and amount of cortical gray matter loss can be inferred from the scatter plots in Figure 4.

As far as age effects are concerned, Lim and Spielman (25) recently reported a trend of reduced NAA levels in the gray matter of healthy elderly when compared with the levels in nonelderly control subjects, which raises the possibility that NAA levels in gray matter may be reduced during normal aging. Therefore, age-related changes in NAA levels may skew results between groups if the groups are not carefully matched in terms of age. In this study, there were no such age-related changes in either AD patients or control subjects. In addition, we tested whether differences in NAA levels between the groups remained statistically significant after adjustment for the age difference and found no contribution from age. Taken together, these results imply that the abnormal NAA levels in AD patients cannot be explained simply in terms of the different age distribution of AD patients and control subjects in this study.

Finally, the contrast between gray and white matter is typically superior on heavily T1-weighted MR images compared with that on T2-weighted images, such as were acquired in this study. Mis-classification of gray and white matter may have affected the calculation of percentage of gray matter and the tissue composition of the imaging voxels. However, at the time of this study, the segmentation software was limited to the processing of T2-weighted images only. Since then, we have developed software to process both T1- and T2-weighted images (37) and have found no statistically significant differences between the two methods as regards the gray and white matter calculations.

Notwithstanding the limitations discussed above, our present results agree with previous observations of reduced levels of NAA in patients with AD, verify that these metabolite changes are independent of variations in the composition of MR spectroscopic imaging voxels, and show that changes in NAA levels correlate with severity of dementia. However, NAA measurements in the frontoparietal brain are of limited use for premorbid diagnosis of AD because of the overlap with such values in healthy elderly persons. Nevertheless, the additional information obtamed with H-1 MR spectroscopic imaging may improve our understanding of the pathologic processes that underlie Alzheimer disease.

Abbreviations

AD, Alzheimer disease; CSF, cerebrospinal fluid; MMSE, Mini-Mental State Examination; NAA, *N*-acetyl aspartate; PET, positron emission tomography.

Acknowledgments

We thank Patricia Gill, BA, for recruitment of the control subjects, James A. Mastrianni, MD, and Kate Skinner, MD, for referrals of patients with Alzheimer disease, and Morton Lieberman, PhD, Director at the University of California at San Francisco Alzheimer Center, for his collaboration throughout this work. We are grateful to Sean Steinman, BSc, for his excellence in performing the MR imaging and MR spectroscopic imaging examinations and for part of the data processing.

References

1. Jernigan TL, Salmon DP, Butters N, Hesselink JR. Cerebral structure on MRI. II. Specific changes in Alzheimer's and Huntington's diseases. Biol Psychiatry 1991;29:68–81. [PubMed: 1825793]
2. Luxenberg JS, Haxby JV, Creasey H, Sundaram M, Rapoport SI. Rate of ventricular enlargement in dementia of the Alzheimer type correlates with rate of neuropsychological deterioration. Neurology 1987;37:1135–1140. [PubMed: 3496557]
3. Tanabe J, Amend D, Schuff N, et al. Tissue segmentation of the brain in Alzheimer's disease. AJNR 1997;18:115–123. [PubMed: 9010529]

4. Kesslak JP, Nalcioglu O, Cotman CW. Quantification of magnetic resonance scans for hippocampal and parahippocampal atrophy in Alzheimer's disease. Neurology 1991;41:51–54. [PubMed: 1985296]
5. Jagust WJ. Functional imaging patterns in Alzheimer's disease: relationships to neurobiology. Ann NY Acad Sci 1996;777:30–36. [PubMed: 8624103]
6. Terry RD, Peck A, DeTeresa R, Schechter R, Horoupian DS. Some morphometric aspects of the brain in senile dementia of the Alzheimer type. Ann Neurol 1981;10:184–192. [PubMed: 7283403]
7. Urenjak J, Williams SR, Gadian DG, Noble M. Specific expression of *N*-acetylaspartate in neurons, oligodendrocyte-type-2 astrocyte progenitors, and immature oligodendrocytes in vitro. J Neurochem 1992;59:55–61. [PubMed: 1613513]
8. Meyerhoff DJ, MacKay S, Constans JM, et al. Axonal injury and membrane alterations in Alzheimer's disease suggested by in vivo proton magnetic resonance spectroscopic imaging. Ann Neurol 1994;36:40–47. [PubMed: 8024260]
9. MacKay S, Meyerhoff DJ, Constans JM, Norman D, Fein G, Weiner MW. Regional gray and white matter metabolite differences in subjects with AD, with subcortical ischemic vascular dementia, and elderly controls with 1H magnetic resonance spectroscopic imaging. Arch Neurol 1996;53:167–174. [PubMed: 8639067]
10. MacKay S, Ezekiel F, Di Sclafani V, et al. Alzheimer disease and subcortical ischemic vascular dementia: evaluation by combining MR imaging segmentation and H-1 MR spectroscopic imaging. Radiology 1996;198:537–545. [PubMed: 8596863]
11. McKhann, G.; Drachman, D.; Folstein, M.; Katzman, R.; Price, D.; Stadlan, EM. Clinical diagnosis of Alzheimer's disease: report of the NINCDS-ADRDA Work Group under the auspices of Department of Health and Human Services Task Force on Alzheimer's Disease; Neurology. 1984. p. 939-944.
12. Folstein MF, Folstein SE, McHugh PR. Mini-mental state: a practical method for grading cognitive state of patients for the clinician. J Psychiatr Res 1975;12:189–198. [PubMed: 1202204]
13. Maudsley AA, Matson GB, Hugg JW, Weiner MW. Reduced phase encoding in spectroscopic imaging. Magn Reson Med 1994;31:645–651. [PubMed: 8057817]
14. Maudsley AA, Lin E, Weiner MW. Spectroscopic imaging display and analysis. Magn Reson Imaging 1992;10:471–485. [PubMed: 1406098]
15. Moats RA, Ernst T, Shonk TK, Ross BD. Abnormal cerebral metabolite concentrations in patients with probable Alzheimer disease. Magn Reson Med 1994;32:110–115. [PubMed: 8084225]
16. Christiansen P, Schlosser A, Henriksen O. Reduced *N*-acetylaspartate content in the frontal part of the brain in patients with probable Alzheimer's disease. Magn Reson Imaging 1995;13:457–462. [PubMed: 7791555]
17. Birken DL, Oldendorf WH. *N*-acetylaspartic acid. Neurosci Biobehav Rev 1989;13:23–31. [PubMed: 2671831]
18. De Stefano N, Matthews PM, Arnold DL. Reversible decreases in *N*-acetylaspartate after acute brain injury. Magn Reson Med 1995;34:721–727. [PubMed: 8544693]
19. Block W, Traeber F, Kuhl CK, et al. 1H-MR spectroscopic imaging in patients with clinically diagnosed Alzheimer's disease. ROFO 1995;163:230–237. [PubMed: 7548870]
20. Ernst T, Chang L, Melchor R, Mehringer CM. Frontotemporal dementia and early Alzheimer disease: differentiation with frontal lobe H-1 MR spectroscopy. Radiology 1991;203:829–836. [PubMed: 9169712]
21. Huang, W.; Ibanez, V.; Chang, L. Brain metabolite quantitation in Alzheimer disease using ^{1}H MR spectroscopy: correlation with disease severity (abstr); Proceedings of the Fifth Meeting of the International Society for Magnetic Resonance in Medicine; Berkeley, Calif: International Society for Magnetic Resonance in Medicine; 1997. p. 298
22. Strittmatter WJ, Roses AD. Apolipoprotein E and Alzheimer's disease. Ann Rev Neurosci 1996;19:53–77. [PubMed: 8833436]
23. Nitsch R, Pittas A, Blusztajn JK, Slack BE, Growdon JH, Wurtman RJ. Alterations of phospholipid metabolites in postmortem brain from patients with Alzheimer's disease. Ann NY Acad Sci 1991;640:110–113. [PubMed: 1663712]
24. Hetherington H, Pan JW, Mason GF, et al. Quantitative ^{1}H spectroscopic imaging of human brain at 4.1-T using image segmentation. Magn Reson Med 1996;36:21–29. [PubMed: 8795016]

25. Lim KO, Spielman DM. Estimating NAA in cortical gray matter with applications for measuring changes due to aging. Magn Reson Med 1997;37:372–377. [PubMed: 9055227]
26. Constans JM, Meyerhoff DJ, Gerson J, et al. H-1 MR spectroscopic imaging of white matter signal hyperintensities: Alzheimer disease and ischemic vascular dementia. Radiology 1995;197:517–523. [PubMed: 7480705]
27. Ende G, Laxer K, Knowlton RC, et al. Temporal lobe epilepsy: bilateral hippocampal metabolite changes revealed at proton MR spectroscopic imaging. Radiology 1997;202:809–818. [PubMed: 9051038]
28. Schuff N, Amend D, Ezekiel F, et al. Changes of hippocampal *N*-acetyl aspartate and volume in Alzheimer's disease: a proton MR spectroscopic imaging and MRI study. Neurology 1997;49:1513–1521. [PubMed: 9409338]
29. Schuff, N.; Weiner, MW. Investigation of metabolite changes in cortex and neocortex of healthy elderly by multislice ^{1}H MR spectroscopic imaging (abstr); Proceedings of the Fourth Meeting of the International Society for Magnetic Resonance in Medicine; Berkeley, Calif: International Society for Magnetic Resonance in Medicine; 1996. p. 1213
30. Duyn JH, Gillen J, Sobering G, van Zijl PC, Moonen CT. Multisection proton MR spectroscopic imaging of the brain. Radiology 1993:277–282. [PubMed: 8511313]
31. Hetherington H, Mason GF, Pan JW, et al. Evaluation of cerebral gray and white matter metabolite differences by spectroscopic imaging at 4.1T. Magn Reson Med 1994;33:565–571. [PubMed: 7808257]
32. Tedeschi G, Bertolino A, Lundborn N, et al. Cortical and subcortical chemical pathology in Alzheimer's disease as assessed by multislice proton magnetic resonance spectroscopic imaging. Neurology 1996;47:696–704. [PubMed: 8797467]
33. Miller BL, Moats RA, Shonk T, Ernst T, Woolley S, Ross BD. Alzheimer disease: depiction of increased cerebral *myo*-inositol with proton MR spectroscopy. Radiology 1993;187:433–437. [PubMed: 8475286]
34. Bruhn H, Weber T, Thorwirth V, Frahm J. In-vivo monitoring of neuronal loss in Creutzfeldt Jakob disease by proton magnetic resonance spectroscopy (letter). Lancet 1991;337:1610–1611. [PubMed: 1675739]
35. Shonk TK, Moats RA, Gifford P, et al. Probable Alzheimer disease: diagnosis with proton MR spectroscopy. Radiology 1995;195:65–72. [PubMed: 7892497]
36. Posse S, Schuknecht B, Smith ME, et al. Short echo time proton MR spectroscopic imaging. J Comput Assist Tomogr 1993;17:1–14. [PubMed: 8380426]
37. Tanabe J, Ezekiel F, Jagust WJ, Schuff N, Fein G. A volumetric method for evaluating magnetization transfer ratio of tissue categories: application to white matter signal hyperintensities in the elderly. Radiology 1997;204:570–575. [PubMed: 9240555]

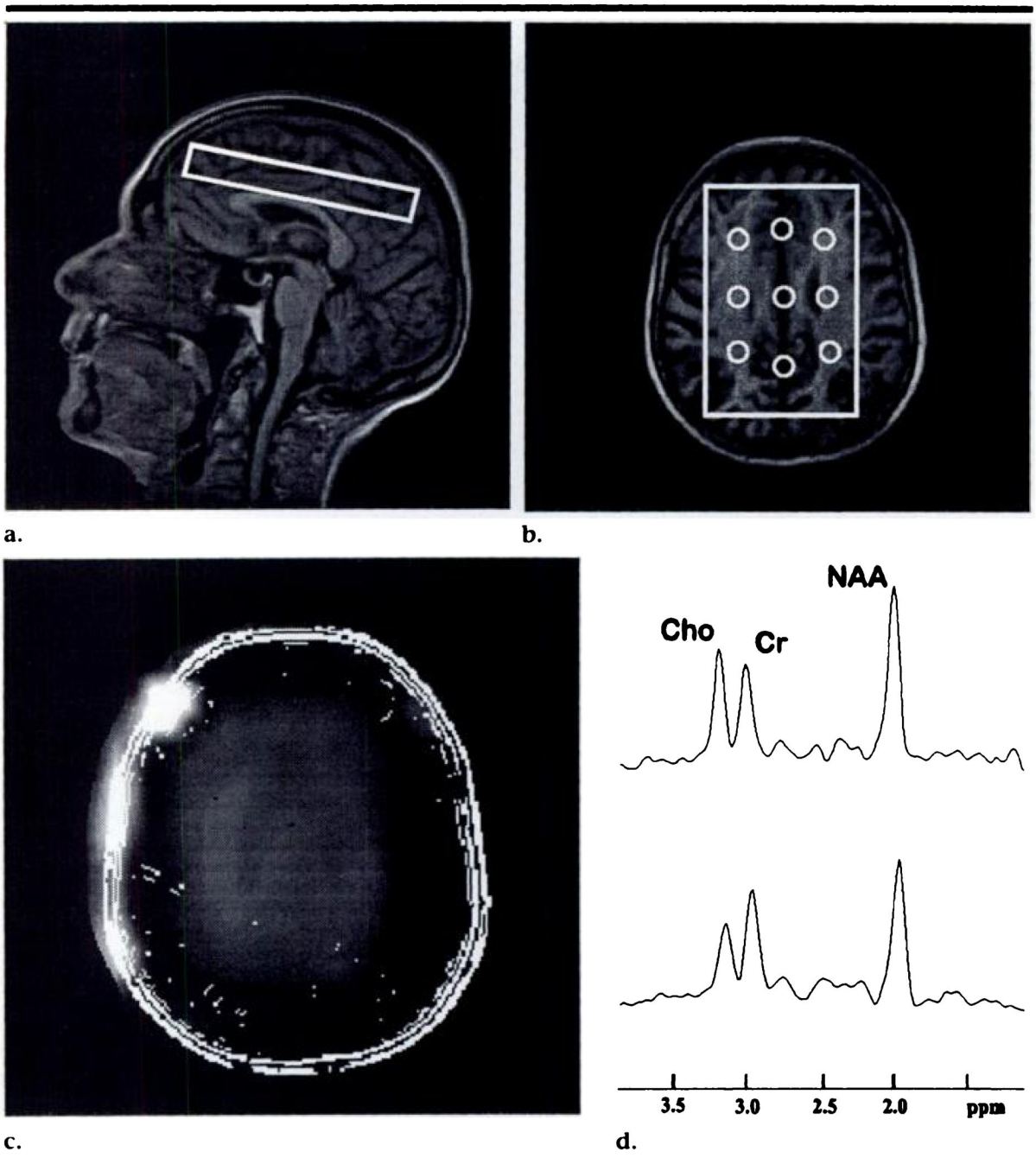

Figure 1.

(a) Sagittal fast low-angle shot (240/6) and **(b)** axial magnetization-prepared rapid gradient-echo (9.7/4) MR images in a 74-year-old control subject show the outlines of the point-resolved spectroscopic volume and a typical position in the frontoparietal region of the brain. The regions from which MR spectroscopic imaging voxels were selected for the spectral analysis and their approximate size are indicated in **a**. **(c)** MR metabolite image of NAA, limited to the sensitive area of the point-resolved spectroscopic volume. Outlines of the anatomic MR image are superimposed on the MR metabolite image for better anatomic reference. Note the different fields of view used for the anatomic and metabolite images. **(d)** Representative H-1 MR spectra

are shown from posterior centrum semiovale (top) and posterior mesial cortex (bottom). *Cho* = choline, *Cr* = creatine.

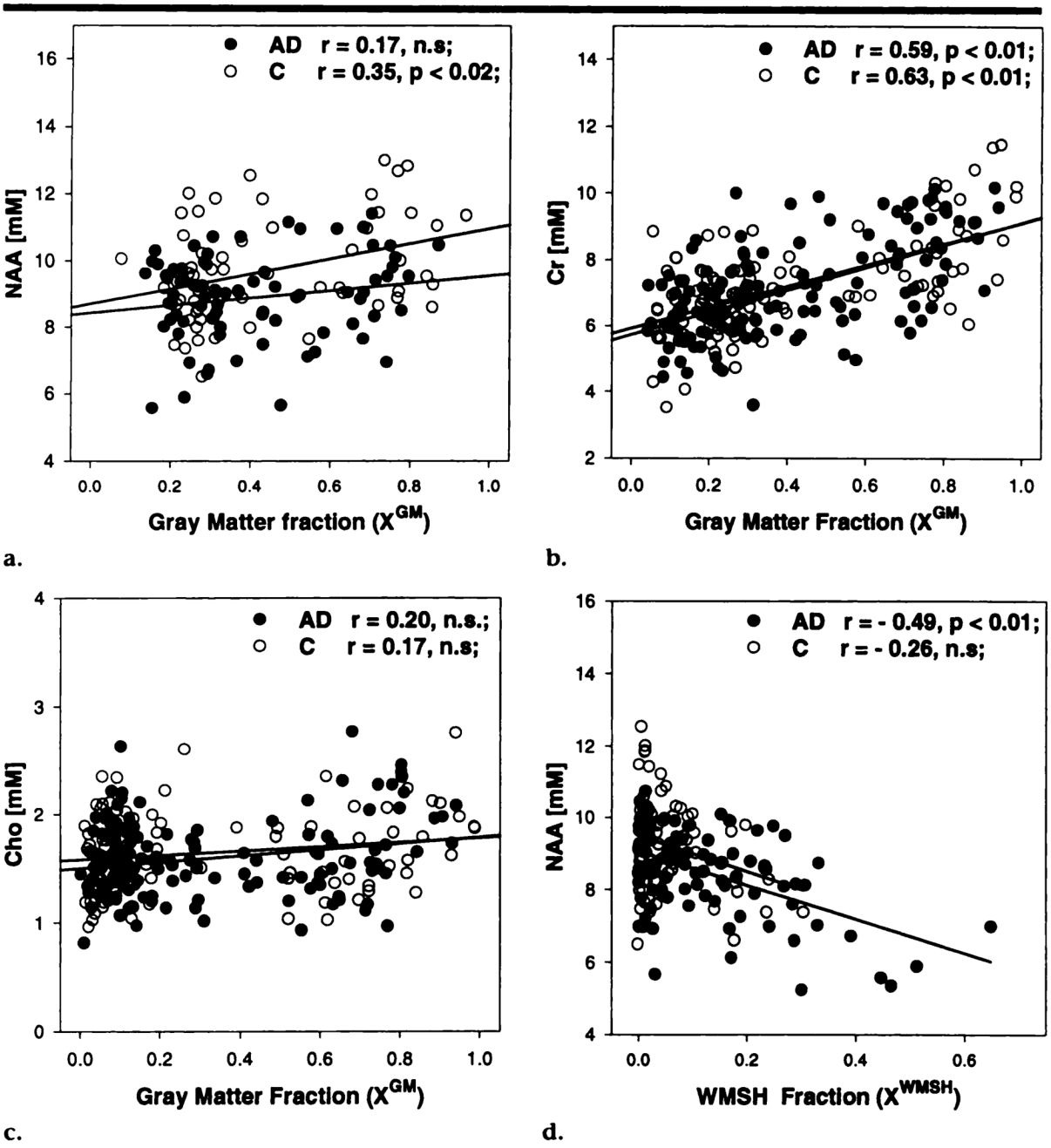

Figure 2.

Linear regression plots of volume-corrected metabolite concentrations versus tissue composition in MR spectroscopic imaging voxels in patients with AD (●) and in control subjects *(C*, O), with the predicted values (lines) for the respective parameters. **(a)** NAA, **(b)** creatine (*Cr*), and **(c)** choline (*Cho*) concentrations are plotted against the gray matter tissue fraction of MR spectroscopic imaging voxels from mesial cortex. **(d)** NAA concentration is plotted against the tissue fraction of hyperintense white matter (*WMSH*) in MR spectroscopic imaging voxels in centrum semiovale white matter. mM = mmol/L, *n.s* = not statistically significant.

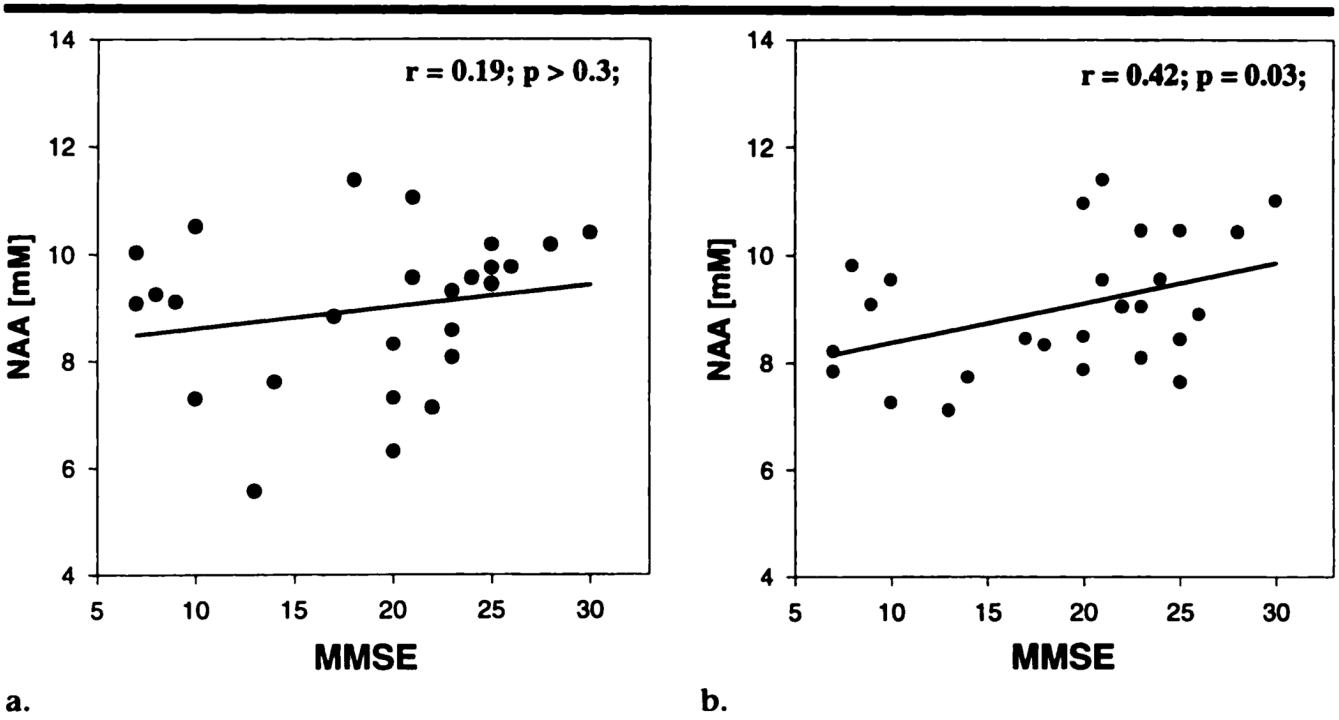

Figure 3.
Linear regression plots of volume-corrected NAA levels in **(a)** frontal mesial cortex and **(b)** posterior mesial cortex of AD patients as a function of MMSE scores. mM = mmol/L.

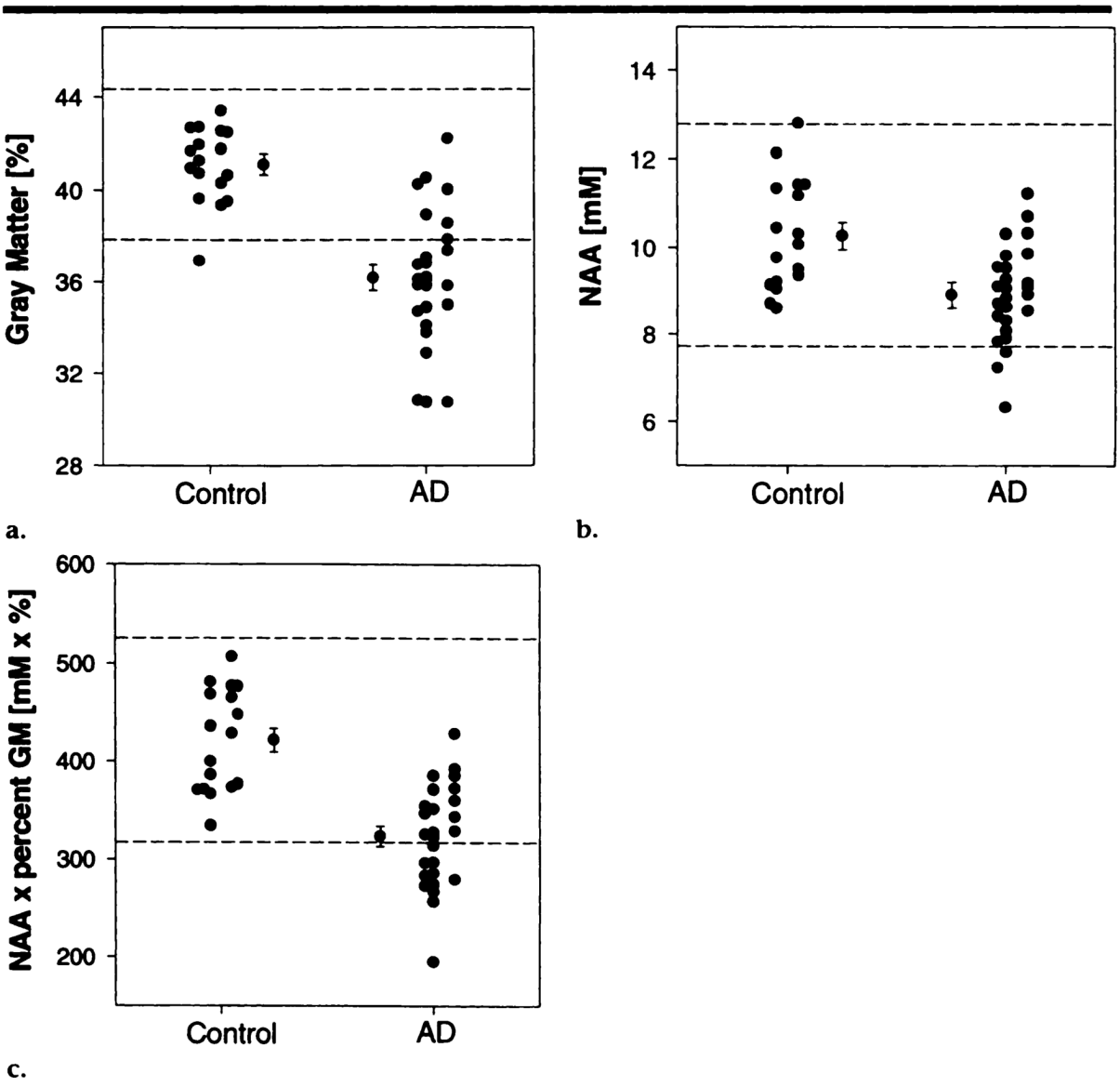

Figure 4.

Distribution in control subjects and AD patients of **(a)** percentage of cortical gray matter, **(b)** volume-corrected NAA level in mesial cortex, and **(c)** the product of percentage of cortical gray matter (*GM*) and volume-corrected NAA level in mesial cortex. Data points with an error bar indicate group means ± the standard error of the mean. For each group (control and AD) data points on the left indicate results in women, and those on the right indicate results in men. Dashed lines = 95% confidence interval in control subjects. mM = mmol/L.

TABLE 1

Clinical Characteristics of Patients with AD and Control Subjects

Characteristic	AD Patients	Control Subjects	*P* Value
No. of individuals			
Study population	28	22	NA
Age-matched subset	17	1 7	NA
Mean age (y)			
Study population*	76.6 ± 7.9	67.9 ± 7.3	.002
Age-matched subset*	73.0 ± 8.0	69.5 ± 7.6	.2
Age range (y)			
Study population	51–87	52–85	NA
Age-matched subset	51–83	52–85	NA
No. of women/men			
Study population	19/9	10/12	NA
Age-matched subset	13/4	10/7	NA
Amount of education (y)			
Study population*	14.1 ± 3.9	16.4 ± 1.4	.1
Age-matched subset*	14.3 ± 2.9	16.1 ± 2.2	.1
Duration of symptoms (y)			
Study population*	4.3 ± 2.3	NA	NA
Age-matched subset*	3.5 ± 2.3	NA	NA
Mean MMSE score			
Study population*	19.1 ± 6.9	29.3 ± 1.0	.001
Age-matched subset*	20.6 ± 6.3	29.5 ± 0.9	.001
MMSE score range			
Study population	8–30	27–30	NA
Age-matched subset	8–30	28–30	NA

Note.—NA = not applicable.

*Data are means ± 1 standard deviation.

TABLE 2

Volume-corrected Concentrations of NAA, Choline, and Creatine in the Age-matched Subset of the Study Population

Brain Structure and Individual	Brain Region		
	Frontal	**Middle**	**Posterior**
	NAA (mmol/L)		
Mesial cortex			
Patients	8.6 ± 0.4	9.3 ± 0.3	9.4 ± 0.3
Control subjects	10.0 ± 0.4	9.7 ± 0.4	10.5 ± 0.4
Difference (%)	−14.0*	−4.1	−10.4*
Centrum semiovale			
Patients	8.3 ± 0.3	9.7 ± 0.3	8.9 ± 0.2
Control subjects	9.2 ± 0.2	9.6 ± 0.2	9.5 ± 0.3
Difference (%)	−9.8†	1.0	−6.3
	Creatine (mmol/L)		
Mesial cortex			
Patients	8.5 ± 0.3	8.1 ± 0.2	8.1 ± 0.3
Control subjects	8.7 ± 0.3	7.3 ± 0.3	8.1 ± 0.3
Difference (%)	−2.3	10.9	0.0
Centrum semiovale			
Patients	6.4 ± 0.2	6.2 ± 0.2	6.7 ± 0.2
Control subjects	6.5 ± 0.3	6.1 ± 0.2	6.7 ± 0.2
Difference (%)	−1.5	1.6	0.0
	Choline (mmol/L)		
Mesial cortex			
Patients	1.8 ± 0.3	1.5 ± 0.2	1.3 ± 0.2
Control subjects	1.8 ± 0.2	1.6 ± 0.2	1.4 ± 0.2
Difference (%)	0.0	−6.2	−7.1
Centrum semiovale			
Patients	1.6 ± 0.2	1.5 ± 0.1	1.3 ± 0.1
Control subjects	1.7 ± 0.2	1.6 ± 0.2	1.3 ± 0.1
Difference (%)	−5.8	−6.2	0.0

Note.—Data are means ± 1 standard error of the mean, unless otherwise indicated.

* Difference between patients and control subjects was statistically significant ($P < .03$).

† Difference between patients and control subjects was statistically significant ($P < .003$).

TABLE 3

Tissue Composition of MR Spectroscopic Imaging Voxels in the Age-matched Subset of the Study Population

Brain Structure	Frontal Brain		Middle Brain		Posterior Brain	
	AD Patients	Control Subjects	AD Patients	Control Subjects	AD Patients	Control Subjects
			NAA			
Mesial cortex						
Gray matter	73.1 ± 2.8*	84.0 ± 2.9*	64.4 ± 1.8	64.3 ± 2.4	68.4 ± 2.4*	77.5 ± 2.2*
White matter	26.9 ± 2.8*	15.9 ± 2.8*	35.1 ± 1.8	35.7 ± 2.4	30.9 ± 2.4*	22.4 ± 2.2*
Hyperintense white matter	0.0 ± 0.3	0.1 ± 0.3	0.5 ± 0.1†	0.0 ± 0.2†	0.7 ± 0.4	0.1 ± 0.1
Centrum semiovale						
Gray matter	16.1 ± 1.9	16.4 ± 2.0	10.4 ± 1.7†	6.9 ± 0.7†	27.7 ± 1.8	28.5 ± 1.8
White matter	67.8 ± 1.9	76.3 ± 2.0	65.9 ± 1.7†	70.1 ± 0.7†	66.3 ± 1.8	68.1 ± 1.8
Hyperintense white matter	16.1 ± 2.5‡	7.3 ± 1.3‡	23.7 ± 2.0	23.0 ± 2.7	6.0 ± 1.6†	3.4 ± 1.5†
			Creatine			
Mesial cortex						
Gray matter	72.8 ± 2.6*	83.6 ± 2.3*	65.2 ± 1.5	64.5 ± 2.3	67.4 ± 1.8*	75.0 ± 2.2*
White matter	27.2 ± 2.6*	16.4 ± 2.3*	34.4 ± 1.5	35.5 ± 2.3	32.2 ± 1.8*	24.7 ± 2.2*
Hyerintense white matter	0.0 ± 0.2	0.0 ± 0.1	0.4 ± 0.2†	0.0 ± 0.2†	0.4 ± 0.3	0.3 ± 0.2
Centrum semiovale						
Gray matter	16.1 ± 1.6	14.2 ± 1.6	11.6 ± 2.1††	6.2 ± 07†	29.2 ± 1.7	27.4 ± 1.5
White matter	63.7 ± 1.6	76.3 ± 1.6	60.2 ± 2.1†	68.1 ± 0.7†	61.8 ± 1.7	68.9 ± 1.5
Hyperintense white matter	20.2 ± 3.2‡	**9.5** ± 1.4‡	28.2 ± 3.4	25.7 ± 2.6	9.0 ± 2.2†	3.7 ± 1.3†
			Choline			

Brain Structure	Frontal Brain		Middle Brain		Posterior Brain	
	AD Patients	Control Subjects	AD Patients	Control Subjects	AD Patients	Control Subjects
Mesial cortex						
Gray matter	74.1 ± 2.3*	83.4 ± 2.4*	65.5 ± 1.5	64.4 ± 2.3	65.9 ± 1.9*	75.0 ± 2.2*
White matter	25.9 ± 2.3*	16.6 ± 2.4*	34.0 ± 1.5	35.6 ± 2.3	33.6 ± 1.9*	24.8 ± 2.2*
Hyperintense white matter	0.0 ± 0.2	0.0 ± 0.2	0.5 ± 0.3†	0.0 ± 0.2†	0.5 ± 0.3	0.2 ± 0.1
Centrum semiovale						
Gray matter	17.1 ± 2.0	14.0 ± 1.6	11.5 ± 2.0†	6.1 ± 0.7†	28.0 ± 1.6	27.4 ± 1.5
White matter	63.2 ± 2.0	76.4 ± 1.6	60.1 ± 2.0†	67.9 ± 0.7†	62.2 ± 1.6	68.9 ± 1.5
Hyperintense white matter	19.7 ± 3.2‡	9.6 ± 1.4‡	28.4 ± 3.5	26.0 ± 2.7	9.8 ± 2.3†	3.7 ± 1.2†

Note.—Data are expressed as the percentage ± standard error of the mean of total tissue content enclosed in an MR spectroscopic imaging voxel.

*Difference between patients and control subjects was statistically significant ($P < .005$).

†Difference between patients and control subjects was statistically significant ($P < .05$).

‡Difference between patients and control subjects was statistically significant ($P < .0001$).

TABLE 4

Volume-corrected Concentration of NAA in Brain Regions of 28 AD Patients 22 Control Subjects and 22 Control Subjects

	Brain Region		
Brain Structure and Individual	**Frontal**	**Middle**	**Posterior**
Mesial cortex			
Patients*	8.8 ± 0.3	9.3 ± 0.2	9.2 ± 0.2
Subjects*	9.9 ± 0.3	9.6 ± 0.4	10.2 ± 0.3
Difference(%)	−11.1†	−3.1	−9.8†
Centrum semiovale			
Patients*	8.2 ± 0.2	9.5 ± 0.3	8.7 ± 0.2
Subjects*	9.1 ± 0.2	9.5 ± 0.2	9.3 ± 0.3
Difference (%)	−9.9	0.0	−6.4

*Data are concentration in millimoles per liter (± standard error of the mean) of NAA.

†Difference between patients and subjects was statistically significant ($P < .02$).

TABLE 5

Tissue Composition of MR Spectroscopic Imaging Voxels in 28 AD Patients and 22 Control Subjects

	Frontal Brain		Middle Brain		Posterior Brain	
Brain Structure	**AD Patients**	**Control Subjects**	**AD Patients**	**Control Subjects**	**AD Patients**	**Control Subjects**
Mesial cortex						
Gray matter	73.2 ± 2.6*	84.1 ± 2.9*	65.1 ± 1.7	65.6 ± 2.2	66.7 ± 1.8*	74.7 ± 2.1*
White matter	26.8 ± 2.6*	15.9 ± 2.8*	34.4 ± 1.7	34.4 ± 2.2	32.8 ± 1.8*	25.0 ± 2.1
Hyperintense white matter	0.0 ± 0.2	0.1 ± 0.3	0.5 ± 0.3	0.0 ± 0.2	0.5 ± 0.4	0.3 ± 0.2
Centrum semiovale						
Gray matter	17.1 ± 1 .7	15.2 ± 1 .6	11.4 ± 1.9*	6.7 ± 0.7*	29.6 ± 1.5	27.6 ± 1.4
White matter	64.1 ± 1.7	76.3 ± 1.6	61.4 ± 1.7*	68.9 ± 0.7*	62.3 ± 1.5	69.0 ± 1.4
Hyperintense white matter	18.8 ± 3.0†	8.5 ±1.3†	27.2 ± 3.3	24.4 ± 2.6	8.1 ± 2.1‡	3.3 ± 1.2‡

Note.—Results in this table are from voxels in regions that correspond to Table 4. Data are expressed as the percentage ± standard error of the mean of total tissue content enclosed in an MR spectroscopic imaging voxel.

*Difference between patients and control subjects was statistically significant ($P < .005$).

†Difference between patients and control subjects was statistically significant ($P < .0001$).

‡Difference between patients and control subjects was statistically significant ($P < .05$).